

Magnetic fields around late-type stars using H_2O maser observations

W.H.T. Vlemmings¹, H.J. van Langevelde² and P.J. Diamond¹

¹ Jodrell Bank Observatory, The University of Manchester, Macclesfield, Cheshire SK11 9DL, U.K e-mail: wouter@jb.man.ac.uk

² Joint Institute for VLBI in Europe, Radiosterrenwacht Dwingeloo, Postbus 2, 7990 AA, Dwingeloo, the Netherlands

Abstract. We present the analysis of the circular polarization, due to Zeeman splitting, of the H_2O masers around a sample of late-type stars to determine the magnetic fields in their circumstellar envelopes (CSEs). The magnetic field strengths in the H_2O maser regions around the Mira variable stars U Ori and U Her are shown to be several Gauss while those of the supergiants S Per, NML Cyg and VY CMa are several hundred mG. We also show that large scale magnetic fields permeate the CSE of an evolved star; the polarization of the H_2O masers around VX Sgr reveals a dipole field structure. We shortly discuss the coupling of the magnetic field with the stellar outflow, as such fields could possibly be the cause of distinctly aspherical mass-loss and the resulting aspherical planetary nebulae.

Key words. masers – polarization – stars: circumstellar matter – stars: magnetic fields – stars: supergiants – stars: Miras

1. Introduction

The exact role of magnetic fields in the mass loss mechanism and the formation of CSEs around late-type stars is still unclear but could be considerable. The study of several maser species found in CSEs has revealed important information about the strength and structure of magnetic fields throughout the envelopes surrounding the late-type stars. At distances from the central star of up to several thousands of AU, measurements of the Zeeman effect on OH masers indicate magnetic fields strengths of a few milliGauss (e.g. Szymczak & Cohen 1997; Masheder et al. 1999). Additionally, weak alignment with the

CSE structure is found (e.g. Etoaka & Diamond 2004). Observations of SiO maser polarization have shown highly ordered magnetic fields close to the central star, at radii of 5-10 AU where the SiO maser emission occurs (e.g. Barvainis, McIntosh, & Predmore 1987; Kemball & Diamond 1997). When interpreting the circular polarization of the SiO masers as standard Zeeman splitting, the magnetic field strength determined from these observations could be up to several tens of Gauss. However, a non-Zeeman interpretation can explain the observations by magnetic field strengths of only several tens of milliGauss (Wiebe & Watson 1998). Recently, high circular polarization of circumstellar H_2O masers was

Send offprint requests to: W.Vlemmings

observed for a small sample of late-type stars (Vlemmings, Diamond, & van Langevelde 2002; Vlemmings & van Langevelde 2005, hereafter V02 and V05). H_2O masers occur at intermediate distances in the CSE, in gas that is a factor of 10–1000 more dense than the gas in which OH masers occur. Here we discuss the results of the H_2O maser observations and their possible role in shaping the CSEs.

2. Observations

The observations were performed at the NRAO¹ Very Long Baseline Array (VLBA). The average beam width is $\approx 0.5 \times 0.5$ mas at the frequency of the $6_{16} - 5_{23}$ rotational transition of H_2O , 22.235 GHz. We used 4 baseband filters of 1 MHz width, which were overlapped to get a velocity coverage of ≈ 44 km/s, covering most of the velocity range of the H_2O masers. The data were correlated multiple times. The initial correlation was performed with modest ($7.8 \text{ kHz} = 0.1 \text{ km s}^{-1}$) spectral resolution, which enabled us to generate all 4 polarization combinations (RR, LL, RL and LR). Two additional correlator runs were performed with high spectral resolution ($1.95 \text{ kHz} = 0.027 \text{ km s}^{-1}$) which therefore only contained the two polarization combinations RR and LL. This was necessary to be able to detect the signature of the H_2O Zeeman splitting in the circular polarization data and to cover the entire velocity range of the H_2O masers. The data analysis path is described in detail in V02.

2.1. Sample

Our sample consists of the 2 Mira variable stars U Her and U Ori and the 4 supergiants VX Sgr, S per, NML Cyg and VY CMa. Observations were also performed on the Mira R Cas but the H_2O masers were not detected. U Her, S Per, VY CMa and NML Cyg are discussed in detail in V02; U Ori, VX SGr and a second epoch of

U Her observations are presented in V05. The stellar sample is listed in Table 1.

3. Results

The magnetic field observed in the H_2O maser regions of our sample is given in table 1. As we only observe the component along the line of sight at the location of the brightest maser features, the magnetic field values are determined from the maximum of the measured values. We determined the magnetic field strength from the observed circular polarization using both an LTE and non-LTE analysis as described in V02. Because the non-LTE method, using the radiative transfer equations from Nedoluha & Watson (1992), provided the best fit, we adopt the non-LTE magnetic field strength values as the true values. The LTE values are typically $\sim 40\%$ higher. Fig. 1 shows several examples of observed total power and circular polarization spectra for VX Sgr. For none of the stars in our sample were we able to detect any significant linear polarization above a limit of $\sim 0.02\%$ for the strongest maser features and a few % for most of the weakest.

3.1. Special case: VX SGr

The rich H_2O maser structure around VX Sgr for the first time enabled us to study the morphology of the magnetic field in the maser region in detail. The maser shell of VX Sgr has been studied extensively with MERLIN and VLA observations (e.g. Lane 1984; Chapman & Cohen 1986; Zell & Fix 1996; Trigilio, Umana, & Cohen 1998). The recent observations of Murakawa et al. (2003, hereafter M03) indicate that the H_2O masers arise in a thick shell between 100 AU and 325 AU from the star. The H_2O maser shell shows a clear elliptical asymmetry which was modelled in M03 as a spheroidal maser distribution intersected with an under-dense biconical region. In our observations we see a clear transition between a negative magnetic field in the S-E to a positive magnetic field in the N-W. We managed to fit a dipole magnetic field to our H_2O maser magnetic field observations with the results shown in Fig. 2.

¹ The National Radio Astronomy Observatory is a facility of the National Science Foundation (NSF) operated under cooperative agreement by Associated Universities Inc.

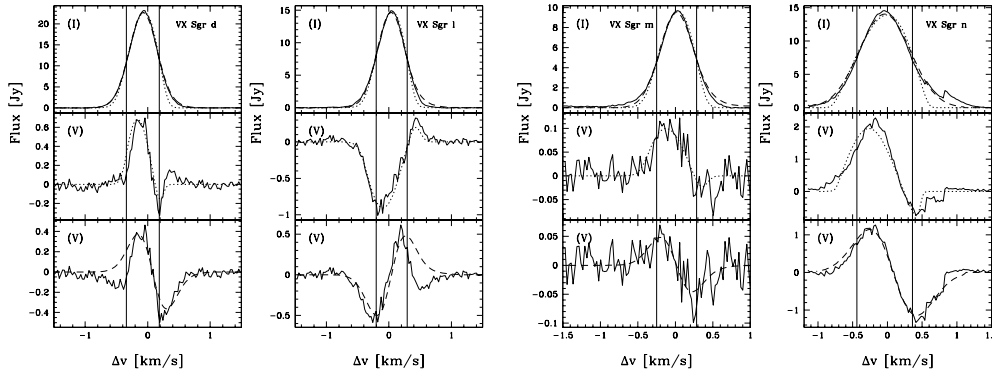


Fig. 1. Examples of the total power (I) and circular polarization (V) spectra for several of the H_2O maser features around VX Sgr. The bottom panel shows the best fitting synthetic V-spectrum produced by the standard LTE Zeeman interpretation (dashed line). The middle panel shows the best non-LTE model fit (dotted line). The corresponding total power fits are shown in the top panel. The V-spectra in the lower two panels are adjusted by removing a scaled down version of the total power spectrum which is different for the LTE and non-LTE fits. The solid vertical lines show the expected position of the minimum and maximum of the V-spectrum in the general LTE interpretation. The magnetic field strengths along the maser line of sight determined from these spectra are -469 ± 60 , 966 ± 120 , -167 ± 87 and -4082 ± 305 respectively.

Table 1. Observed Stars

| Star | Type | RA (J2000) (^h ^m ^s) | Dec (J2000) ([°] ['] ^{''}) | Distance (pc) | Period (days) | V_{rad} (km/s) | $B_{\text{H}_2\text{O}}$ (G) |
|---------|------------|--|--|------------------|------------------|----------------------------|---------------------------------|
| U Her | Mira | 16 25 47.4713 | +18 53 32.867 | 277 | 406 | -14.5 | ~ 1.5 |
| U Ori | Mira | 05 55 49.1689 | +20 10 30.687 | 300 | 368 | -38.1 | ~ 3.5 |
| VX Sgr | Supergiant | 18 08 04.0485 | -22 13 26.614 | 1700 | 732 | 5.3 | $\sim 0.5 - 4$ |
| S Per | Supergiant | 02 22 51.72 | +58 35 11.4 | 1610 | 822 | -38.1 | ~ 0.15 |
| NML Cyg | Supergiant | 20 46 25.7 | +40 06 56 | 1220 | 940 | 0.0 | ~ 0.18 |
| VY CMa | Supergiant | 07 22 58.3315 | -25 46 03.174 | 1500 | 2000 | 22.0 | ~ 0.5 |

The best fitted model is a dipole with its magnetic axis pointed toward us at an inclination angle $i = 40 \pm 5^\circ$, and a position angle of $\Theta = 220 \pm 10^\circ$. The fitted values are remarkably consistent with the values found for the magnetic field determined from OH masers, as well as with the orientation angle determined from the H_2O maser distribution in M03 and Marvel (1996). As a result of our fit, we find that the magnetic field strength at the surface of VX Sgr

corresponds to $B \approx 2.0 \pm 0.5$ kG, consistent with the OH and SiO maser observations (Barvainis, McIntosh, & Predmore 1987). This is the first detection of a large scale magnetic field in a circumstellar H_2O maser region.

4. Discussion

The observed magnetic field strengths on the H_2O masers are consistent with the results for the other maser species assuming a $B \propto r^\alpha$ de-

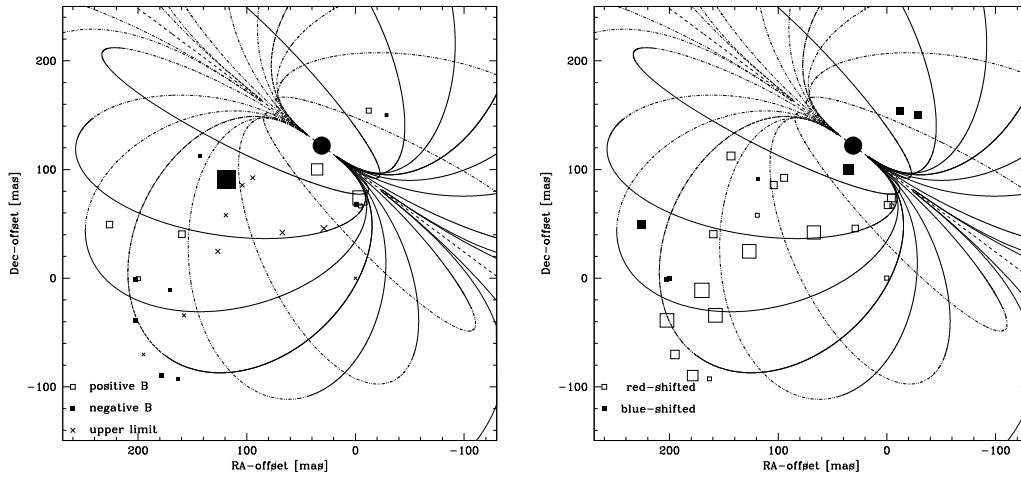


Fig. 2. The best fitted dipole magnetic field for the H₂O maser observations around VX Sgr (denoted by the solid circle). (left) The distribution of the H₂O maser features indicating the measured magnetic field strengths. Open symbols denote a positive magnetic field while the closed symbols correspond to a negative magnetic field. The crosses represent the upper limits. The symbols have been scaled relative to the magnetic field strength. (right) The distribution of the H₂O maser features indicating the velocity structure of the maser features. The open symbols are the red-shifted features and the solid symbols are the blue-shifted features. The size indicates the velocity difference with the stellar velocity ($v_{\text{rad}} = 5.3 \text{ km s}^{-1}$)

pendence of the field strength on the distance to the star. As the magnetic field strength determined for the SiO, H₂O and OH maser features depends on the angle between the magnetic field and the maser propagation axis, it is difficult to exactly determine the value of α . In Fig. 3 we show the relation between the magnetic field strength and the distance from the star for the stars in our sample. The points for the H₂O masers are drawn at the outer radius of the maser region which is an upper limit. Extrapolating the observed magnetic field strengths to the stellar surface, we find that Mira variable stars have surface field strengths up to several times 10^2 G , while supergiant stars have fields of the order of 10^3 G . Such high magnetic field strengths indicate that the standard Zeeman interpretation of the SiO maser polarization is most likely correct.

The origin of the strong, large scale magnetic fields around evolved stars remains a topic of debate. The generation of an axisymmetric magnetic field requires a magnetic dynamo in the interior of the star. Several models have been discussed in the literature that

include the interaction between the differential rotation and turbulence in the convection zone around the degenerated core (e.g. Blackman et al. 2001). However, a supergiant core is supposedly not degenerate. A dynamo driven by the differential rotation between the contracting non-degenerate core and the expanding outer envelope has also been shown to also be able to generate strong magnetic fields (Uchida & Bappu 1982). In alternative models, a strong magnetic field can be generated when the star is spun up by a close binary. The sources in our sample do not however, show any indication of binarity, although this cannot be ruled out.

The magnetic field strength of several Gauss measured in the H₂O maser region implies that the magnetic pressure dominates the thermal pressure of the circumstellar gas throughout a large part of the CSE of both regular AGB stars and supergiants. The effects of magnetic fields on the stellar outflow and the shaping of the distinctly aspherical PNe have been discussed in several papers (e.g. Pascoli 1987; Chevalier & Luo 1994;

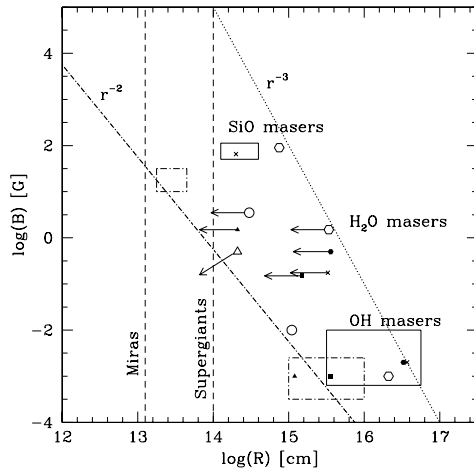


Fig. 3. Magnetic field strength, B , as function of distance, R , from the centre of the star. Dashed-dotted boxes are the estimates for the magnetic fields in the OH and SiO maser regions of Mira stars, solid boxes are those for the supergiants. The dashed-dotted line indicates a solar-type magnetic field and the dotted line indicates the dipole field. The solid symbols are the stars observed during our first observations (U Her: triangles; S Per: squares; VY CMa: crosses and NML Cyg: hexagonals). The open symbols indicate the stars of the sample observed during our second observations (U Her: triangle; VX Sgr: hexagonal and U Ori: circle). Note that the open triangle only indicates the upper limit determined for the most recent observation of U Her. Also note that the magnetic field strength observed on the OH masers of U Ori is larger than the typically observed fields for Mira variables. The dashed lines represent estimates of the stellar radius.

García-Segura 1997). Strong, large scale, magnetic fields around AGB stars could directly affect the fast wind that shapes the PN or could have shaped the initial matter distribution during the slow wind. For instance, a dipole field has been shown to be able to create an equatorial, possibly warped, disk (Matt et al. 2000). Interactions with a warped disk have been shown to be able to form multipolar PNe (Icke 2003).

5. Conclusions

We have measured the strong magnetic field around a sample of late-type stars using observations of the circular polarization of their H₂O masers. Observations of VX Sgr also indicate that the magnetic field has a dipole shape that can be responsible for shaping the outflow. For the lower mass late-type stars the magnetic field can be the cause of aspherical PNe.

References

- Barvainis, R., McIntosh, G., & Predmore, C. R. 1987, *Nature*, 329, 613
- Blackman, E. G., et al. 2001, *Nature*, 409, 485
- Chapman, J. M. & Cohen, R. J. 1986, *MNRAS*, 220, 513
- Chevalier, R. A. & Luo, D. 1994, *ApJ*, 421, 225
- Etoka, S. & Diamond, P. 2004, *MNRAS*, 348, 34
- García-Segura, G. 1997, *ApJ*, 489, L189
- Icke, V. 2003, *A&A*, 405, L11
- Kemball, A. J. & Diamond, P. J. 1997, *ApJ*, 481, L111
- Lane, A. P. 1984, *IAU Symp. 110: VLBI and Compact Radio Sources*, 110, 329
- Mashedier, M. R. W., et al. 1999, *New Astronomy Review*, 43, 563
- Matt, S., et al. 2000, *ApJ*, 545, 965
- Marvel, K. B. 1996, Ph.D. Thesis, New Mexico State Univ.
- Murakawa, K., et al. 2003, *MNRAS*, 344, 1 (M03)
- Nedoluha, G. E. & Watson, W. D. 1992, *ApJ*, 384, 185
- Pascoli, G. 1987, *A&A*, 180, 191
- Szymczak, M. & Cohen, R. J. 1997, *MNRAS*, 288, 945
- Trigilio, C., Umana, G., & Cohen, R. J. 1998, *MNRAS*, 297, 497
- Uchida, Y. & Bappu, M. K. V. 1982, *Journal of Astrophysics and Astronomy*, 3, 277
- Vlemmings, W. H. T., Diamond, P. J., & van Langevelde, H. J. 2002, *A&A*, 394, 589 (V02)
- Vlemmings, W. H. T., van Langevelde, H. J., & Diamond, P. J. 2005, *A&A*, 434, 1029 (V05)
- Wiebe, D. S. & Watson, W. D. 1998, *ApJ*, 503, L71

Zell, P. J. & Fix, J. D. 1996, AJ, 112, 252